

Studies of Ozone-Sensitized Low- and High-Temperature Oxidations of Diethyl Carbonate

Published as part of *The Journal of Physical Chemistry virtual special issue "Emily A. Carter Festschrift"*.

Hao Zhao,* Shixiang Liu, Chao Yan, Can Huang, Yongfeng Qi, Feng Zhang, and Yiguang Ju



Cite This: *J. Phys. Chem. A* 2021, 125, 1760–1765



Read Online

ACCESS |



Metrics & More

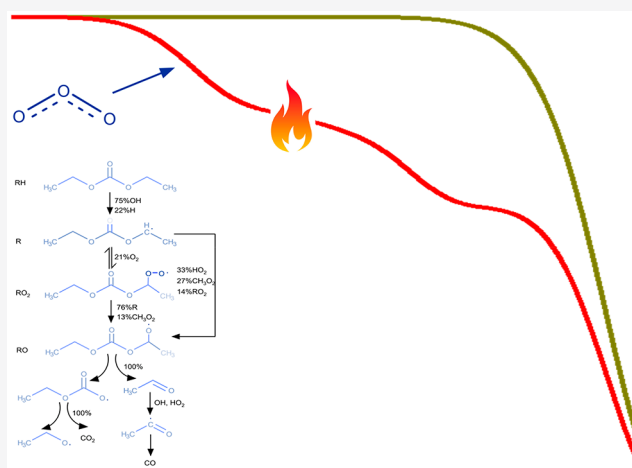


Article Recommendations



Supporting Information

ABSTRACT: Diethyl carbonate (DEC) oxidation with different levels of O₃ addition was performed in an atmospheric laminar flow reactor from 400 to 850 K. Experimental results showed that, without O₃ addition, the oxidation of DEC began from 650 K with no low-temperature reactivity, while with O₃ addition the low-temperature chemistry of DEC was observed from 450 K. A DEC/O₃ kinetic model was developed, and the model predictions agreed with the experimental data reasonably well with a slight overprediction of DEC oxidation between 550 and 750 K. The low-temperature chemistry of DEC with O₃ addition was described in the reaction pathway of DEC. It was found that O₃ assisted the low-temperature oxidation of DEC mainly through the production of the active O: atom instead of the direct reaction with the fuel molecule. The present work indicated that the Li-ion battery degradation at 400–500 K might result from the low-temperature chemistry of DEC with active oxygen supplies from the cathode metal oxide materials or from singlet O₂ during the battery discharge process. This article used O₃ to mimic the oxidizing environment in the Li-ion battery by providing active atomic oxygen. It provided insights into the chemically sensitized gas-phase low-temperature chemistry of DEC and explained the mechanism of battery degradation involving the low-temperature oxidation at the electrolyte solvent and the cathode interface from 400 to 500 K.



INTRODUCTION

The increase in the number of electrical vehicles (EVs) provides a great opportunity to combine electric transportation and smart mobility together with energy storage. In particular, the lithium ion battery (LIB) with high energy density is a promising candidate for next-generation energy storage and transportation systems. The 2018, the EV outlook published by the International Energy Agency (IEA) forecasted that global EVs powered by LIB will surpass 228 million units by 2030, equivalent to 17 100 gigawatt hours (GWH) of power capacity.^{1–3} The world demand of LIB with high energy density is unprecedented.

Unfortunately, LIB cathode materials normally contain low nickel contents (30–60%) due to the high fire propensity of high-nickel cathode materials. For example, the increase in the nickel/cobalt ratio in nickel, cobalt, and manganese (NCM) cathode materials from 3:3 to 8:1 results in lower thermal stability and a lower ignition onset temperature, accompanied by a large amount of oxygen gas released and vigorous reactions with electrolyte solvents.^{1,4–6} Under some extreme conditions such as overcharging, overdischarging, and internal short circuits, the battery temperature can increase dramati-

cally beyond the safe operating rating, which often initiates a series of exothermal reactions. These reactions further lead to a quick temperature increase, electrolyte oxidation, and even fires. The degradation phenomenon of the Li-ion battery under abuse conditions is called the thermal runaway.⁴ Recently, by using online electrochemical mass spectrometry (OEMS), Jung et al.⁷ and Gueguen et al.⁸ showed that, during the initial charging cycles, molecular oxygen was released from the NCM surface lattice at high degrees of delithiation. They explained that the gas-phase oxidation between electrolyte solvents and O₂ leads to the battery thermal runaway. Hwang et al.⁹ explored the effect of the transition metal on the thermal runaway with oxygen revolution by using real-time electron microscopy. On top of that, Berkes et al. performed high-

Received: October 4, 2020

Revised: January 19, 2021

Published: February 1, 2021

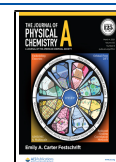


Table 1. Experimental Conditions

case	DEC (%)	O ₂ (%)	O ₃ (%)	Ar (%)	He (%)	flow rate (L/min)	residence time (s)	temp range (K)
1	0.5000	2.5000	0.000	2.0000	95.0000	2.25	1.47–0.65	400–850
2	0.5000	2.4646	0.0236	2.0000	95.0118	2.25	1.47–0.65	400–850
3	0.5000	2.4192	0.0539	2.0000	95.0270	2.25	1.47–0.65	400–850

precision long-term cycling tests using online continuous flow differential electrochemical mass spectrometry.¹⁰ CO₂, H₂, and C₂H₄ products were observed, which is directly evident in solvent oxidation reactions. However, electrolyte solvents, such as dimethyl carbonate (DMC), diethyl carbonate (DEC), and ethylene carbonate (EC), do not react with O₂ below 650 K in the gas phase, while a Li-ion battery often fails at 400–500 K. This implies that, instead of oxidation by molecular oxygen, some stronger oxidizers, such as atomic oxygen from the cathode material, may react with the electrolyte solvents at low temperatures and accelerate the thermal runaway. More importantly, Wandt et al.¹¹ successfully detected singlet oxygen formation inside Li-ion batteries, which provides evidence that the reaction between singlet O₂ and electrolyte solvents is important. However, many aspects related to the initial temperature rise and interactions between electrolyte solvent and oxidizers, such as singlet O₂, atomic oxygen, and metal oxide in the cathode material, are still not well understood.

Ozone is a strong oxidizer and decomposes to molecular oxygen and atomic oxygen quickly above 400 K. O₃ is known to accelerate low-temperature fuel oxidations and sustain cool flames.^{12–14} The present study aims to use O₃ to mimic the oxidizing environment in a Li-ion battery by providing active atomic oxygen, sensitizing the low-temperature oxidation of DEC (an electrolyte solvent representative), and understanding the thermal runaway involved in electrolyte at low temperature (400–500 K). The experiment of DEC oxidation with and without O₃ addition is performed in an atmospheric laminar flow reactor from 400 to 850 K. The mole fractions of DEC, O₂, O₃, CH₂O, CH₃CHO, C₂H₄, CO, CO₂, and C₂H₅OH are in situ quantified by using molecular beam mass spectrometry (MBMS) and microgas chromatography (μ -GC) simultaneously. A detailed kinetic model is developed on the basis of Nakamura's model¹⁵ and the Princeton O₃ submechanism¹² to predict major and intermediate species profiles and to capture the O₃ sensitization characteristics.

EXPERIMENTAL METHODS AND KINETIC MODELS

The experiments were performed in a fused silica flow reactor covered by a stainless-steel jacket with a regulated electrical resistance heating system. The jacket was surrounded by insulating materials, allowing an operating temperature of up to 1300 K. The laminar flow reactor was a cylindrical quartz tube of 17 mm inner diameter and 320 mm length. Reactants were supplied through an inlet channel of 100 mm length and 2 mm inner diameter with no recirculation zone at the reactor entrance. The schematic of the reactor and its coupling with the sonic probes is given in detail.^{12,13} The volumetric flow rates of Ar, He, and O₂ were regulated by mass flow controllers (MKS, 0.5% uncertainty). Ozone was produced by an ozone generator (Ozone Solutions, TG-20) from a pure oxygen stream and mixed with Ar and He as a primary stream of gases at room temperature (293 K). The ozone concentration in the mixture was measured in a UV absorption cell using a deuterium lamp (Oriel) and a spectrometer with a charge-coupled device (CCD) detector (Ocean Optics, USB 2000+).

The detailed procedure is described in refs 12 and 16. The absorption spectra from 260 to 280 nm were used to extract the concentration. The O₃ concentration was measured right after the ozone generator, at the inlet and the outlet of the flow reactor at room temperature with fixed flow conditions. The difference in O₃ concentrations was less than 2%, which showed that there was no significant decomposition of O₃ in the gas line and the reactor at room temperature. Liquid DEC was regulated and delivered by a syringe pump (Harvard Apparatus, PHD 22/2000) to a vaporizer. A secondary stream of He carried gaseous DEC from the vaporizer up to the entrance of the reactor after preheating and then was mixed with the primary stream of gases. The temperature profile along the reactor was measured from 400 to 850 K by using the experimental gas mixture (DEC/O₂/O₃/Ar/He) and was plotted in Figure S1 of the Supporting Information, in which the temperature variation was within ± 5 K. Samples of the reacting mixture were taken with two sonic probes for simultaneous analyses via MBMS and μ -GC.

An electron-ionization MBMS with a mass resolution of $m/\Delta m = 900$ was employed to measure major combustion species at the exit of the flow reactor. Each important species was calibrated directly by a flow of the mixture with a known mole fraction in excess He. The measurement uncertainty was around 10–20%, which was mainly from the species calibration for MBMS and the electron impact (20 ± 1 eV) in MBMS. GC-TCD (Inficon 3000) measurements were also taken to identify and quantify intermediates and products from the exit of the reactor within 5% uncertainty. DEC, O₂, CO, CO₂, O₃, and C₂H₅OH are quantified by using EI-MBMS, while DEC, O₂, CO, CO₂, C₂H₄, CH₂O, and CH₃CHO are quantified by using GC. No secondary reactivities of these stable molecules have been observed in our GC measurements. The details of MBMS and GC are described in refs 17–20.

The experiments were performed under conditions with and without O₃ addition from 400 to 850 K at 1 atm. The inlet volume flow rate was fixed at 2.25 L/min at 293 K, and as such, the residence time in the reactor varied with the reactor temperature (T) through $\tau = (V/v)T_0/T$, where V is the volume of the flow reactor, v is the inlet volume flow rate at room temperature, and T_0 is room temperature (293 K). The experimental residence time was comparable to the calculated characteristic reaction time scale of DEC low-temperature oxidation with O₃ addition in CHEMKIN software.²¹ Species measurements were repeated two times at every experimental condition with a repeatability uncertainty of <2%. The experimental conditions are shown in Table 1.

The DEC/O₃ model in the present work consists of a recently developed DEC model by Nakamura¹⁵ and the Princeton O₃ submechanism.¹² In the O₃ submechanism, the O₃ decomposition reaction and the O₃ reactions with O, H, \cdot OH, HO₂, H₂O, CO, H \cdot CO, \cdot CH₃, and DEC were included. O₃ reactions with other radicals or intermediate species are significantly slower than O₃ decomposition and are not considered in the model development. Simulations were

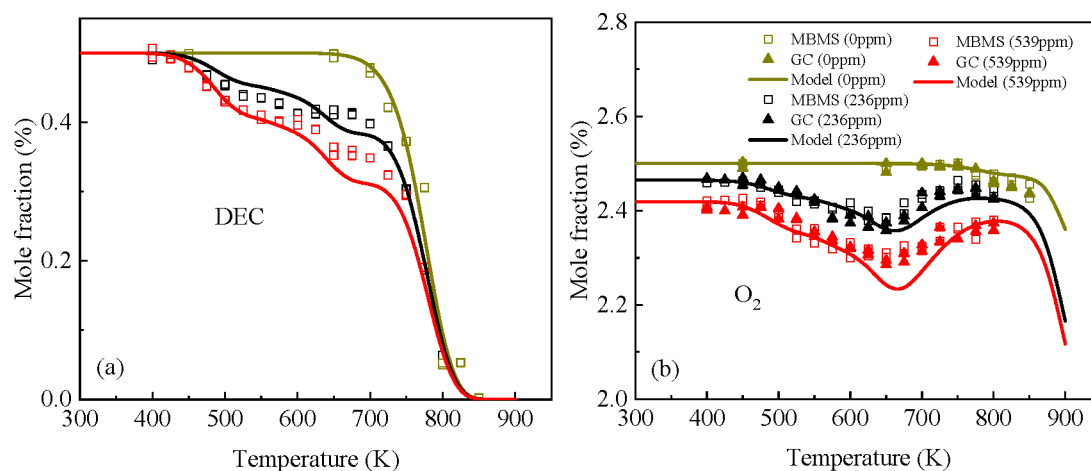


Figure 1. Temperature evolution of DEC (a) and O_2 (b) with different levels of O_3 addition at 1 atm.

performed in the 0-D homogeneous module of CHEMKIN software.²¹

RESULTS AND DISCUSSION

The mole fractions of DEC and O_2 against temperature with different levels of O_3 addition are plotted in Figure 1(a) and (b), respectively. Experimental data in Figure 1(a) and (b) shows that without O_3 addition, the oxidation of DEC begins at 650 K and DEC does not exhibit any low-temperature reactivity. This observation agrees with the literature report.¹⁵ However, with O_3 addition, there is a significant low-temperature oxidation of DEC from 450 K, and the oxidation is accelerated at a higher level of O_3 addition. The DEC/ O_3 model in the present work predicts the oxidation of DEC well without O_3 addition. Under the conditions with O_3 addition, the model captures the low-temperature oxidation of DEC successfully. However, the model overpredicts the DEC and O_2 consumption slightly between 550 and 750 K with 236 and 539 ppm of O_3 addition, exhibiting model uncertainties in the low-temperature pathway of DEC oxidation.

To explain and analyze the low-temperature oxidation of DEC with O_3 addition, the pathway analysis of DEC with 539 ppm O_3 addition is performed at 600 K in Figure 2. The low-temperature oxidation pathway is as follows. DEC produces $C_2H_5OCOOC\cdot HCH_3$ through the H-atom abstraction reaction by O and OH, and $C_2H_5OCOOC\cdot HCH_3$ combines with O_2 and forms $C_2H_5OCOOC\cdot H(OO)\cdot CH_3$. Then, $C_2H_5OCOOC\cdot H(OO)\cdot CH_3$ is formed through the reactions of $C_2H_5OCOOC\cdot HCH_3 + C_2H_5OCOOC\cdot H(OO)\cdot CH_3/HO_2\cdot/CH_3O_2\cdot$. $C_2H_5OCOOC\cdot H(OO)\cdot CH_3$ decomposes to $C_2H_5OCOO\cdot$ and CH_3CHO through β -scission and finally forms CO and CO_2 . Without O_3 addition, DEC shows no low-temperature reactivity due to the large energy barrier of DEC + O_2 . However, with O_3 addition, O_3 decomposes to O and O_2 dramatically above 450 K, and then the active O atom directly participates in the reaction with DEC with a much lower energy barrier and accelerates the DEC low-temperature oxidation. It is noted that the direct reaction between DEC and O_3 does not appear in the reaction pathway of DEC; therefore, O_3 assists the low-temperature oxidation of DEC mainly through the production of an active O atom instead of the direct reaction with the fuel molecule.

Furthermore, the sensitivity analysis of DEC with 539 ppm O_3 addition at 600 K (Figure 3) is conducted to analyze the

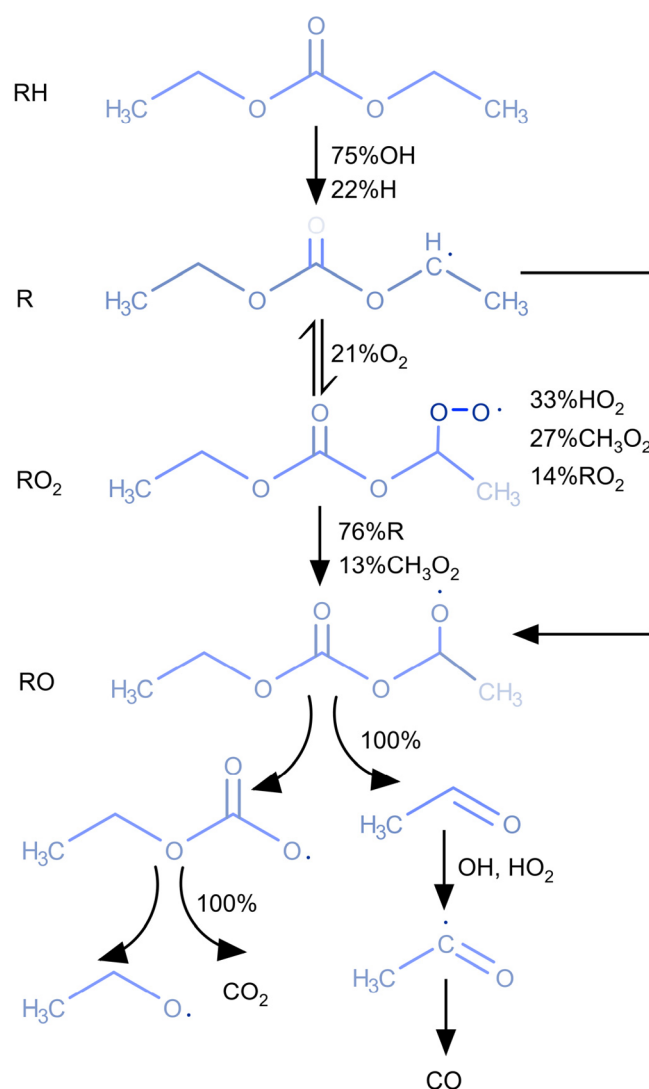


Figure 2. Schematic of the reaction pathway of DEC with 539 ppm O_3 addition at 600 K and 1 atm.

model uncertainty in the temperature range of 550–750 K. The sensitivity for the DEC mole fraction is defined as $sensitivity_{DEC} = (\Delta X_{DEC}/X_{DEC})/(\Delta k_i/k_i)$, where X_{DEC} is the mole fraction of DEC and k_i is the i th reaction's rate constant.

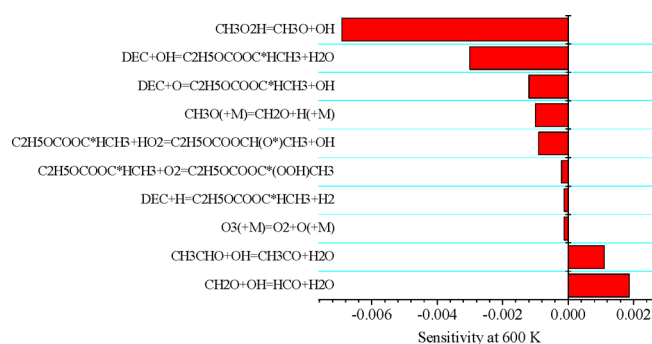


Figure 3. Sensitivity analysis of DEC with 539 ppm O_3 addition at 600 K and 1 atm.

The most sensitive reaction is $CH_3O_2H = CH_3O \cdot + \cdot OH$, in which CH_3O_2H is formed from $CH_3O_2 \cdot$. And then H-atom abstraction reactions of DEC by $\cdot OH/O \cdot /H \cdot$ and reactions involving CH_2O and CH_3CHO are also sensitive. In addition, the reaction of the DEC radical ($C_2H_5OCOOC \cdot HCH_3$) with $HO_2 \cdot$ appears here, which is a key reaction in the formation of small radicals and aldehydes. Among these reaction sets, $CH_3O_2 \cdot$ and CH_2O subchemistry have been well studied and validated in the literature with small rate uncertainties.^{22–26} However, the H-atom abstraction reactions of DEC in the DEC base model¹⁵ were determined by analogy to the H-atom abstractions from ethyl esters.^{27,28} Although the DEC base model has been validated in the high-temperature jet stirred

reactor (JSR) and shock tube experiments,¹⁵ the H-atom abstraction reactions are not validated at temperatures below 700 K. Therefore, more effort is needed for theoretical calculations and experimental validations of these H-atom abstractions reactions. We think that the uncertainties in the H-atom abstraction reactions, especially for $DEC + \cdot OH$, result in the overprediction of DEC consumption at 550–750 K.

Figure 4(a)–(d) depicts the mole fractions of CO, CH_3CHO , CH_2O , and CO_2 , respectively, with different levels of O_3 addition. With O_3 addition, these four species appear from 450 K and exhibit low-temperature oxidation peaks. The model predicts the observed trends in the species profiles reasonably well but overpredicts the production of CH_3CHO significantly. Sensitivity analysis shows that the most sensitive reactions are H-abstraction reactions via $\cdot OH/H \cdot$ and CH_3CHO consumption reactions. In particular, we think that competing reactions $CH_3CHO + \cdot OH = CH_3C \cdot O + H_2O$ and $CH_3CHO + \cdot OH = \cdot CH_3 + HOCHO$ need to be further investigated in the model development.

Figure 5(a)–(c) depicts the mole fractions of C_2H_4 , C_2H_5OH , and O_3 , respectively, with different levels of O_3 addition. In Figure 5(a) and (b), there is no production of C_2H_4 and C_2H_5OH below 650 K in the experiment, indicating that they are not the major products in the low-temperature oxidation of DEC. Therefore, C_2H_4 and C_2H_5OH exhibit little sensitivity to the levels of O_3 addition at low temperature in both experiments and model simulations. In addition, in Figure 5(c), O_3 starts to decompose from 450 K rapidly and the

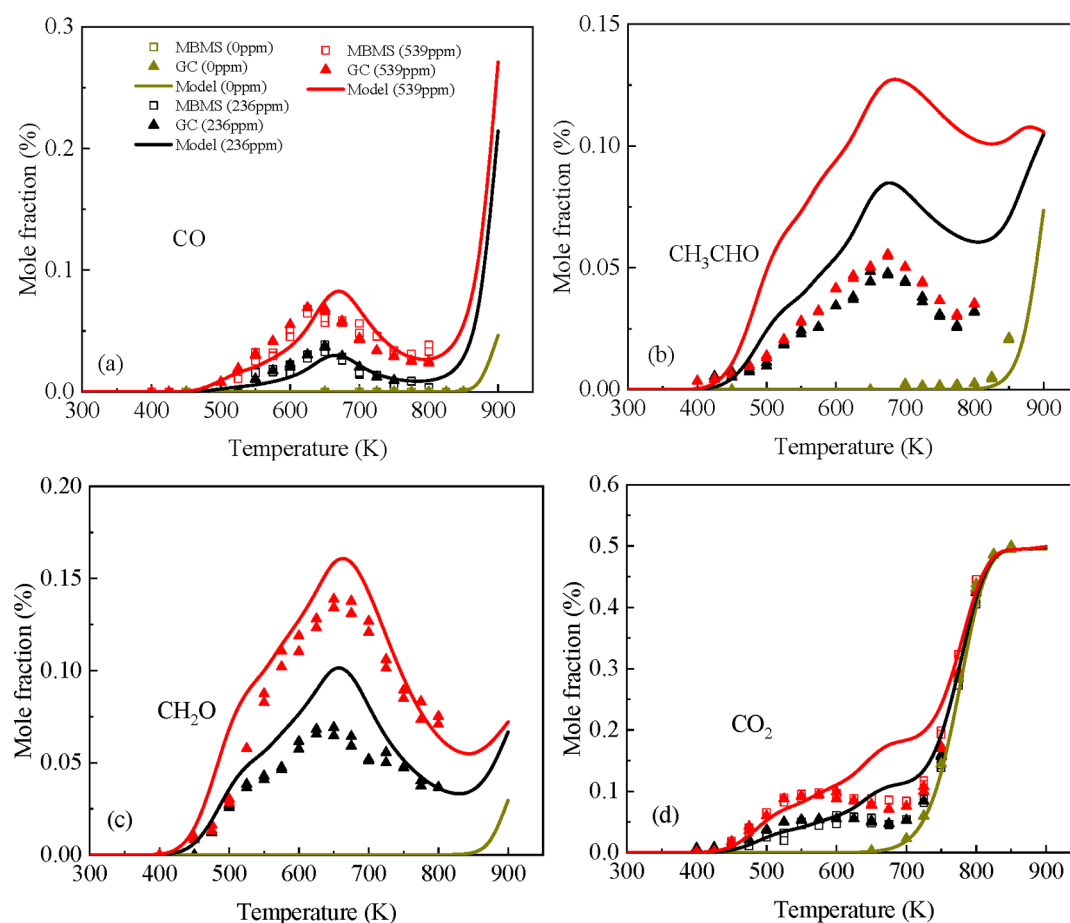


Figure 4. Temperature evolution of CO (a), CH_3CHO (b), CH_2O (c), and CO_2 (d) with different levels of O_3 addition at 1 atm.

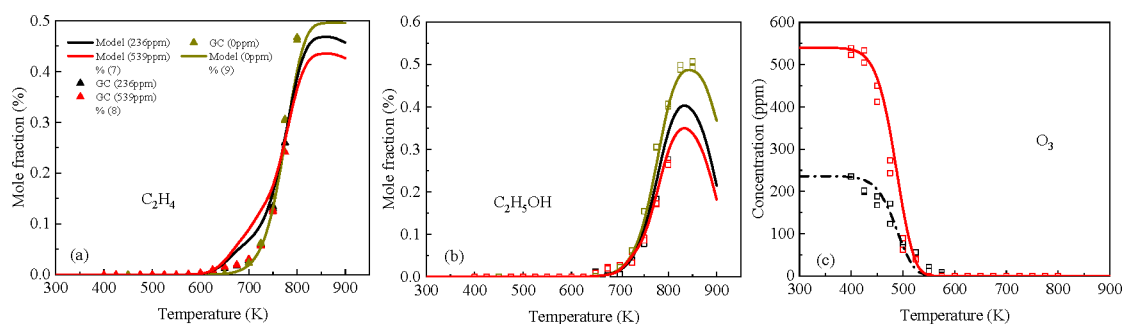


Figure 5. Temperature evolution of C_2H_4 (a), C_2H_5OH (b), and O_3 (c) with different levels of O_3 addition at 1 atm.

model predicts the O_3 mole fraction profile very well, which corresponds to our previous observation.^{12,29} It is interesting that DEC is also dramatically oxidized from 450 K with O_3 addition. It implies that, at low temperatures, DEC is oxidized as soon as O_3 starts to decompose and form an O: atom from 450 K. In other words, the low-temperature chemistry of DEC lies in the introduction of active atomic O:

In the Li-ion battery, DEC, an electrolyte solvent representative, is chemically stable in air below 650 K. However, the battery can still degrade and catch fire at 400–500 K. The present work indicates that this may result from the low-temperature chemistry of DEC with reactive oxygen supplies from the metal oxide cathode materials or singlet O_2 during the battery discharge process. The study of O_3 -assisted DEC oxidation in this article provides insights into the chemically sensitized gas-phase low-temperature chemistry of DEC and the degradation of electrolyte solvents at low temperatures. However, in reality, O_3 may not be produced in the battery charge/discharge process, while DEC may react with surface O: from cathode materials directly. The oxidation mechanism of DEC with surface O: is very different from the gas-phase oxidation in terms of DEC adsorption, metallic reactions on the surface, fuel radical desorption, O_2 desorption, and so forth. Therefore, the heterogenous reaction kinetics of DEC with metallic oxide is greatly needed to help understand the low-temperature oxidation of DEC and the battery thermal runaway. We will study the heterogenous oxidation of DEC and cathode materials in experiments with in situ diagnostics and in molecular dynamics simulations in the future.

CONCLUSIONS

Low-temperature DEC oxidation with different levels of O_3 addition was performed in an atmospheric laminar flow reactor from 400 to 850 K. Experimental results show that, without O_3 addition, the oxidation of DEC begins from 650 K and DEC does not exhibit any low-temperature reactivity, while with O_3 addition, low-temperature chemistry of DEC is observed from 450 K. A DEC/ O_3 kinetic model was developed in this article, and the model prediction agrees reasonably well with the experimental results while slightly overpredicting the DEC oxidation at 550–750 K. The low-temperature chemistry of DEC with O_3 addition was described in the reaction pathway of DEC. It is found that O_3 assists the low-temperature oxidation of DEC mainly through the production of an active O: atom instead of the direct reaction with the fuel molecule. Sensitivity analysis shows that the uncertainties in the H-atom abstraction reactions of DEC may result in the overprediction of DEC consumption.

Although DEC is chemically stable in air below 650 K, the Li-ion battery can still degrade and catch fire at 400–500 K. The present work indicates that it may result from the low-temperature chemistry of DEC with reactive oxygen supplies from the metal oxide cathode materials or singlet O_2 during the battery discharge process. This article uses O_3 to mimic the oxidizing environment in Li-ion batteries by providing active atomic oxygen. It provides insights into the chemically sensitized gas-phase, low-temperature chemistry of DEC and explains the mechanism of battery degradation involving the low-temperature oxidation at the electrolyte solvent and cathode interface at 400–500 K.

ASSOCIATED CONTENT

Supporting Information

The Supporting Information is available free of charge at <https://pubs.acs.org/doi/10.1021/acs.jpca.0c09002>.

Temperature profile along the reactor measured from 400 to 850 K by using the experimental gas mixture (PDF)

DEC/ O_3 coupling mechanism (TXT)

DEC/ O_3 coupling thermodynamic document (TXT)

AUTHOR INFORMATION

Corresponding Author

Hao Zhao – Department of Mechanical and Aerospace Engineering, Princeton University, Princeton, New Jersey 08544-5263, United States; Department of Mechanical Engineering, The Hong Kong Polytechnic University, Hung Hom, Hong Kong; orcid.org/0000-0002-8879-9595; Email: cgsq725525@gmail.com

Authors

Shixiang Liu – Department of Mechanical and Aerospace Engineering, Princeton University, Princeton, New Jersey 08544-5263, United States

Chao Yan – Department of Mechanical and Aerospace Engineering, Princeton University, Princeton, New Jersey 08544-5263, United States; orcid.org/0000-0002-2415-6080

Can Huang – Chair of Technical Thermodynamics, RWTH Aachen University, Aachen 52062, Germany

Yongfeng Qi – Department of Mechanical and Aerospace Engineering, Princeton University, Princeton, New Jersey 08544-5263, United States; orcid.org/0000-0001-7748-5999

Feng Zhang – National Synchrotron Radiation Laboratory, University of Science and Technology of China, Hefei, Anhui 230029, China; orcid.org/0000-0002-9730-8487

Yiguang Ju – Department of Mechanical and Aerospace Engineering, Princeton University, Princeton, New Jersey 08544-5263, United States

Complete contact information is available at:
<https://pubs.acs.org/10.1021/acs.jpca.0c09002>

Notes

The authors declare no competing financial interest.

ACKNOWLEDGMENTS

This work was partially supported by NSF grants CBET 1903362 and 1449314 and the Andlinger Center for Energy and the Environment of Princeton University.

REFERENCES

- (1) Li, M.; Lu, J.; Chen, Z.; Amine, K. 30 years of lithium-ion batteries. *Adv. Mater.* **2018**, *30*, 1800561.
- (2) Goodenough, J. B. How we made the Li-ion rechargeable battery. *Nat. Electron.* **2018**, *1*, 204.
- (3) Abram, C.; Shan, J.; Yang, X.; Yan, C.; Steingart, D.; Ju, Y. Flame aerosol synthesis and electrochemical characterization of ni-rich layered cathode materials for li-Ion batteries. *ACS Appl. Energy Mater.* **2019**, *2*, 1319–1329.
- (4) Wen, J.; Yu, Y.; Chen, C. A review on lithium-ion batteries safety issues: existing problems and possible solutions. *Mater. Express* **2012**, *2*, 197–212.
- (5) Lu, L.; Han, X.; Li, J.; Hua, J.; Ouyang, M. A review on the key issues for lithium-ion battery management in electric vehicles. *J. Power Sources* **2013**, *226*, 272–288.
- (6) Wang, Q.; Ping, P.; Zhao, X.; Chu, G.; Sun, J.; Chen, C. Thermal runaway caused fire and explosion of lithium ion battery. *J. Power Sources* **2012**, *208*, 210–224.
- (7) Jung, R.; Metzger, M.; Maglia, F.; Stinner, C.; Gasteiger, H. A. Oxygen release and its effect on the cycling stability of LiNi_xMn_yCo_zO₂ (NMC) cathode materials for Li-ion batteries. *J. Electrochem. Soc.* **2017**, *164*, A1361–A1377.
- (8) Guéguen, A.; Streich, D.; He, M.; Mendez, M.; Chesneau, F. F.; Novák, P.; Berg, E. J. Decomposition of LiPF₆ in high energy lithium-ion batteries studied with online electrochemical mass spectrometry. *J. Electrochem. Soc.* **2016**, *163*, A1095–A1100.
- (9) Hwang, S.; Kim, S. M.; Bak, S.-M.; Kim, S. Y.; Cho, B.-W.; Chung, K. Y.; Lee, J. Y.; Stach, E. A.; Chang, W. Using real-time electron microscopy to explore the effects of transition-metal composition on the local thermal stability in charged Li_xNi_yMn_zCo_{1-y-z}O₂ cathode materials. *Chem. Mater.* **2015**, *27*, 3927–3935.
- (10) Berkes, B. B.; Jozwiuk, A.; Vračar, M.; Sommer, H.; Brezinsinski, T.; Janek, J. Online continuous flow differential electrochemical mass spectrometry with a realistic battery setup for high-precision, long-term cycling tests. *Anal. Chem.* **2015**, *87*, 5878–5883.
- (11) Wandt, J.; Freiberg, A. S.; Ogródnik, A.; Gasteiger, H. A. Singlet oxygen evolution from layered transition metal oxide cathode materials and its implications for lithium-ion batteries. *Mater. Today* **2018**, *21*, 825–833.
- (12) Zhao, H.; Yang, X.; Ju, Y. Kinetic studies of ozone assisted low temperature oxidation of dimethyl ether in a flow reactor using molecular-beam mass spectrometry. *Combust. Flame* **2016**, *173*, 187–194.
- (13) Guo, H.; Sun, W.; Haas, F. M.; Farouk, T.; Dryer, F. L.; Ju, Y. Measurement of H₂O₂ in low temperature dimethyl ether oxidation. *Proc. Combust. Inst.* **2013**, *34*, 573–581.
- (14) Ju, Y.; Reuter, C. B.; Won, S. H. Numerical simulations of premixed cool flames of dimethyl ether/oxygen mixtures. *Combust. Flame* **2015**, *162*, 3580–3588.
- (15) Nakamura, H.; Curran, H. J.; Córdoba, A. P.; Pitz, W. J.; Dagaut, P.; Togbé, C.; Sarathy, M.; Mehl, M.; Agudelo, J. R.; Bustamante, F. An experimental and modeling study of diethyl carbonate oxidation. *Combust. Flame* **2015**, *162*, 1395–1405.
- (16) Ombrello, T.; Won, S. H.; Ju, Y.; Williams, S. Flame propagation enhancement by plasma excitation of oxygen. Part I: Effects of O₃. *Combust. Flame* **2010**, *157*, 1906–1915.
- (17) Zhao, H.; Wu, L.; Patrick, C.; Zhang, Z.; Rezgui, Y.; Yang, X.; Wysocki, G.; Ju, Y. Studies of low temperature oxidation of n-pentane with nitric oxide addition in a jet stirred reactor. *Combust. Flame* **2018**, *197*, 78–87.
- (18) Zhang, Z.; Zhao, H.; Cao, L.; Li, G.; Ju, Y. Kinetic effects of n-heptane addition on low and high temperature oxidation of methane in a jet-stirred reactor. *Energy Fuels* **2018**, *32*, 11970–11978.
- (19) Zhao, H.; Dana, A. G.; Zhang, Z.; Green, W. H.; Ju, Y. Experimental and modeling study of the mutual oxidation of N-pentane and nitrogen dioxide at low and high temperatures in a jet stirred reactor. *Energy* **2018**, *165*, 727–738.
- (20) Zhao, H.; Yan, C.; Zhang, T.; Ma, G.; Souza, M. J.; Zhou, C.-W.; Ju, Y. Studies of high-pressure n-butane oxidation with CO₂ dilution up to 100 atm using a supercritical-pressure jet-stirred reactor. *Proc. Combust. Inst.*, **2020**, in press. DOI: 10.1016/j.proci.2020.08.047.
- (21) CHEMKIN-PRO, 15112; Reaction Design, Inc.: San Diego, CA, 2011.
- (22) Sangwan, M.; Yan, C.; Chesnokov, E. N.; Krasnoperov, L. N. Reaction CH₃ + CH₃ → C₂H₆ studied over the 292–714 K temperature and 1–100 bar pressure ranges. *J. Phys. Chem. A* **2015**, *119*, 7847–7857.
- (23) Yan, C.; Krasnoperov, L. N. Pressure-dependent kinetics of the reaction between CH₃O₂ and OH: TRIOX formation. *J. Phys. Chem. A* **2019**, *123*, 8349–8357.
- (24) Yan, C.; Kocevská, S.; Krasnoperov, L. N. Kinetics of the reaction of CH₃O₂ radicals with OH studied over the 292–526 K temperature range. *J. Phys. Chem. A* **2016**, *120*, 6111–6121.
- (25) Zhao, H.; Zhang, Z.; Rezgui, Y.; Zhao, N.; Ju, Y. Studies of high pressure 1, 3-butadiene flame speeds and high temperature kinetics using hydrogen and oxygen sensitization. *Combust. Flame* **2019**, *200*, 135–141.
- (26) Zhao, H.; Fu, J.; Haas, F. M.; Ju, Y. Effect of prompt dissociation of formyl radical on 1, 3, 5-trioxane and CH₂O laminar flame speeds with CO₂ dilution at elevated pressure. *Combust. Flame* **2017**, *183*, 253–260.
- (27) Mendes, J.; Zhou, C.-W.; Curran, H. J. Theoretical and kinetic study of the hydrogen atom abstraction reactions of esters with HO₂ radicals. *J. Phys. Chem. A* **2013**, *117*, 14006–14018.
- (28) Mendes, J.; Zhou, C.-W.; Curran, H. J. Theoretical study of the rate constants for the hydrogen atom abstraction reactions of esters with OH radicals. *J. Phys. Chem. A* **2014**, *118*, 4889–4899.
- (29) Zhao, H. Oxidation of hydrocarbons and oxygenated fuels with chemical sensitization by ozone/NO_x/radicals. Ph.D. Thesis, Princeton University, 2019, 22615129.